Experimental methods of the study of vortex structures excited by point injection on the leading edge of the oblique wing

S.N. Tolkachev, V.N. Gorev*, G.M. Zharkova*, V.N. Kovrizhina**
**Khristianovich Institute of Theoretical and Applied Mechanics SB RAS,*
Institutskaya str. 4/1, Novosibirsk 630090

Abstract

The article presents the results of application of thermoanemometry on a curved surface and the liquid crystal thermography to study the stability of the flow on the leading edge of a oblique wing. Quantitative results of the distribution of the velocity perturbation in the boundary layer near the attachment line were obtained with a help of thermoanemometry. A decrease in the stability of the boundary layer of the modified stationary vortex is found. The method of liquid crystal thermography allowed expanding the study area to 70° on both sides of the attachment line, get pictures of disturbed flow visualization for multiple modes of injection, and show the influence of the injection velocity on the size and trajectory of stationary disturbances induced by airjet. Visualization results are consistent with the thermoanemometry.

1. Introduction

1.1. Laminar-turbulent transition on the oblique wing

The boundary layer of oblique wing has a three-dimensional structure and consist of longitudinal and transverse components. Cross-flow velocity profile has an inflection point and thus unstable. Laminar-turbulent transition on a oblique wing occurs in the following scenario: in a favorable pressure gradient near the leading edge in the boundary layer appears cross-flow instability [1, 2], which has a form of longitudinal vortices that modify the mean flow [3, 4]. As a result, the boundary layer flow region appear with inflection points on velocity profiles, that are experiencing secondary high frequency disturbances [5], growing along the stream, which lead to the laminar-turbulent transition.

1.2. Measurement techniques on the leading edge

The leading edge of each wing is a curved surface, the shape of which depends on the selected profile, which greatly complicates its study.
Researchers have different views to choose the profile for the experiment. Some people choose real airfoils, arguing that they are actually used, and therefore of great value. On the other hand, the flow characteristics will be obtained are only for this profile, and it becomes difficult to generalize to the others. The second part of investigators use in experiments swept cylinder, as a first approximation of any leading edge. To prevent separation on the leeward side the plane and turbulators were installed.
Another problem is the measurements on the oblique wing leading edge. Hot-wire measurements require that the sensor wire should be tangent to the surface and have a possibility for measuring only one component of velocity. Two and moreover three-wire sensors have stronger influence on the flow and significantly increases the measurement volume, which is not acceptable for a thin boundary layer near the attachment line. Researchers have a different view on hot-wire technique: some use fixed to the surface hot-wire anemometer sensors [6], the latter use traverse mechanisms [7], the automation of which allows you to receive a large amount of data, but requires a synchronization system and feedback.
We should also highlight the visualization of the flow, as a way of leading edge research. Methods of black-oil visualization and naphthalene sublimation themselves are disturbing because of changing the surface roughness, causing the formation of stationary vortices. Besides, the black-oil visualization method does not allow receiving the information in separation zones, has insufficient sensitivity and is disposable.

The liquid crystal thermography method (LCT) allows the visualization of the distribution of temperature and/or heat flow, which reflects the structure of near-wall flow model of the insulator [8, 9]. It is interactive, allowing you to change the conditions of the experiment, with almost no influence on the surface roughness, but it can have a thermal effect on the flow.

1.3. Blowing

The use of roughness in the experiments on the stability of the boundary layer encounters the next challenge - it is hard to change the size and shape of the roughness during the experiment, and there is a limited set of content. In this situation, it is another attractive way to excite stationary vortices - blowing through the small hole. Experiments [10, 11, 12] confirm the formation of the pair of stationary vortices in the boundary layer after single jet. Because roughness also excites a pair of counter-rotating vortices, it is possible to carry out an analogy between it and the point-blowing. At the same time, blowing is a convenient tool to study the stability of the boundary layer, since it is possible to adjust the speed of injection, simulating roughness of various sizes. Pneumoroute connected to the speaker allows the speaker to introduce high frequency disturbances through the hole regardless of the compressor.
It should be noted that the physics of the excitation of stationary vortices by roughness and airjet differs. The roughness can be modeled by weak blowing. Increase the strength of injection can lead to a complication of the flow pattern.
The aim of this work - to determine the effect of a point blowing on the oblique wing leading edge on the flow and establish its suitability as a source of disturbances, simulating a single roughness using an automated thermoanemometry method and the method of liquid crystal thermography.

2. Investigation of the oblique wing leading edge

2.1.Measurement conditions

Experiment was carried out in a low-turbulent wind tunnel T-324 of the Institute of Theoretical and Applied Mechanics with a cross section of the working section 1000×1000 mm and a length of 4000 mm. The free-stream turbulence level didn't exceed 0.03%. Free-stream velocity in hot-wire measurements was U_∞ = 4.2 m/s, and in the LC thermography was ranged U_∞= 3.4 - 9.4 m/s and monitored by the Prandtl-Pitot tube. The air temperature was 22°C.
In order to improve the quality of visualization, illumination of the working part was supplemented by two halogen lamps with a reflector of 100 watts each. The lamps were positioned so that illumination of the work area on the leading edge wing did not give glare and also not to affect on the flow in the wind tunnel.

2.2. Investigated model

For investigations on the leading edge a swept wing model of 5 mm thick organic glass was made. The chord is c_h = 400 mm, and the swept angle χ = 45°, with a continuously variable angle of attack (**Fig.1**). Because the model is intended only for research at the leading edge, a simple airfoil was chosen, which formed by the cylinder and two planes. Physically, the leading edge of each wing is a second-order approximation cylinder, which allows us to simplify and generalize the results of the experimental measurements on any other profile. To avoid boundary layer separation, causing flow pulsation in the upstream region, for maximum thickening wing (along boundaries between cylinder and plates) turbulators were installed. The disturbances that develop in the working section wall boundary layer cut off by the endplate.
On the leading edge of the oblique wing was the hole with diameter d_{hole} = 0.5 mm, connected to the compressor by pneumoroute. The hole location was chosen to be at the attachment line at zero angle of attack.

2.3. Technique of injecting of controlled disturbances

The disturbance was injected with a help of technique of controlled blowing through the hole (**Fig.1**). Blowing produced by a compressor, the duration defined fast electromagnetic valve synchronized with the recording signal.

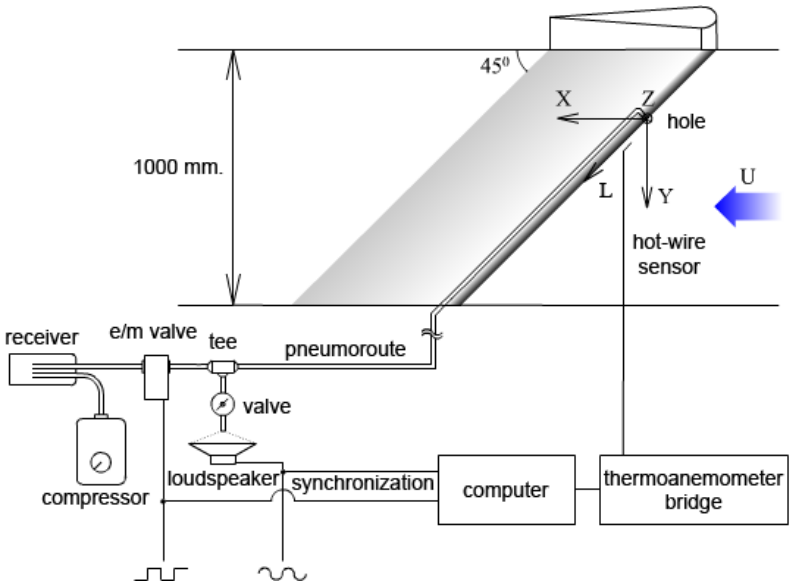

Figure 1: Experimental setup for investigation of airjet influence on the flow near the attachment line using hot-wire measurements.

Valve switching frequency was 0.5 Hz, thus longitudinal disturbances introduced into the boundary layer were quasistationary. We investigated the influence of different blowing velocity. It was realized two regimes of disturbance injection superimposed on the low-frequency blowing: with and without of high-frequency component overlapping. High-frequency perturbations of 110 Hz, 160 Hz and 210 Hz were injected into the flow through tee pneumoroute after electromagnetic valve using a dynamic speaker, according to the method described in [13, 14]. Only difference was that for the generation of longitudinal disturbance used not a loudspeaker, but the compressor (**Fig.1**). By adjusting the angle of attack α near zero reached a different position of point injection d relative to the attachment line, thus the behavior of the studied disturbances could changed.

2.4. Thermoanemometry

Model positioned horizontally (**Fig.1.**). X-axis coordinate system is directed along the flow. Z-axis is vertical and tangent to the wing leading edge. Y-axis is perpendicular to the axes X, Z. The origin of coordinates coincides with the center hole or with the projection of this point on the cylinder axis. Furthermore, use additional axis L, which is directed along the leading edge downstream.

The measurements were made with single-wired constant temperature anemometer. The diameter of the probe wire was 6 microns, in length was about 1 mm. Oscillograms of velocity U (t) at different points in space (x, y, z) were measured and recorded in a computer. Free-stream velocity in the working section of wind tunnel was measured by Pitot - Prandtl nozzle connected to an electronic micromanometer. Hot-wire sensor was calibrated in the free stream in front of the Pitot - Prandtl nozzle at flow rates of $0 \div 6$ m/s, so that the error in determining the average speed was less than 2%. Calibration process and the applied experimental equipment are described in detail in [15].

Oscillogram from the bridge anemometer via an analog-to-digital converter was recorded in the computer. To highlight the low-frequency disturbance to improve the signal-noise ratio used ensemble averaging. To receive distribution of the amplitude and phase of the high-frequency disturbances were using Fourier analysis.

During the measurements used two approaches. First, the measured velocity profile of the boundary layer in the vicinity of the attachment line and velocity profiles to the coordinate Z - tangent to the cylinder (**Fig.2.b**) at different distances from the source of disturbance. Second, a methodology was developed three-dimensional measurements of the velocity fields with rotation sensor anemometer on its axis when passing to the angular coordinate the sensor wire is tangent to the surface of the model (**Fig.2.a**).

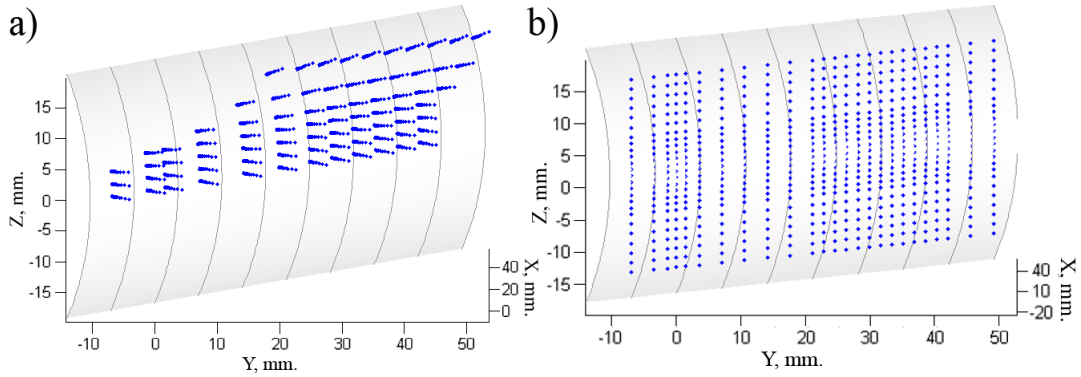

Figure 2: Hot-wire measurement points on the oblique wing leading edge.

2.5. Liquid crystal thermography technique

On the heat transfer from the wall effect dU/dy, where U is the local speed, y is coordinate normal to the wall. By measuring the heat transfer coefficient at each point, you can determine the location of the laminar-turbulent transition, area of the flow separation, the location of stationary disturbances and efficiently monitor their amplitude.

In an aerodynamic experiment liquid crystals can be used for visualization of temperature and shear stress [16]. In our experiments we used liquid-crystal thin-film coatings based on cholesteric liquid crystals insensitive to shear stresses. The fundament of this method is the dependence of wavelength selective reflection of the cholesteric on the temperature. As a result, the color of the film will depend on the temperature and observation angles. With increasing temperature, the coating changes color from brown-red to blue-purple. Using temperature-color and angle-color calibration can be obtained the temperature distribution on the examined surface. The film has a certain temperature range ΔT, beyond which the coating loses its selective reflection. By reducing the operating range, the film becomes more sensitive. Thus, it is necessary for the experiment to find the right parameters of the film. In this case, the operating range of the film was $\Delta T = 3°$.

To study the quasi-stationary flow structure near the wall on the leading edge of the oblique wing by an ohmic heater were implemented constant heat flux boundary conditions. A layer of liquid crystal film was fixed on top of the heater (**Fig.2.**).

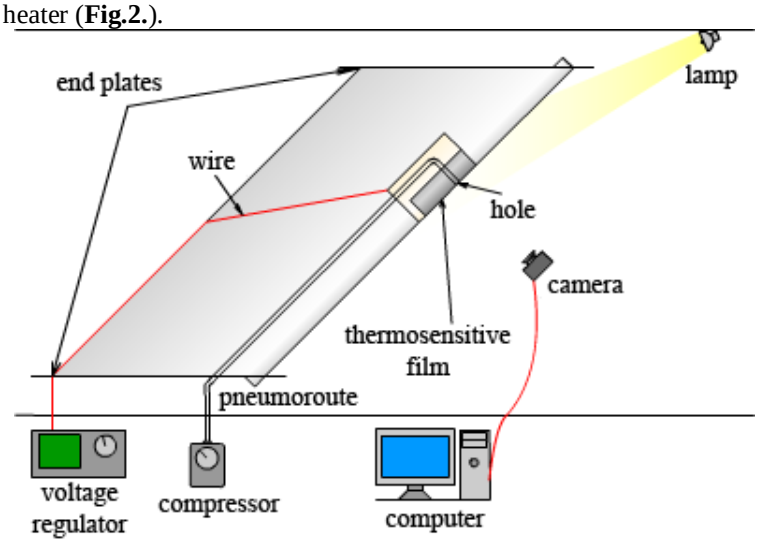

Figure 3: Experimental setup for investigating vortex structure on the oblique wing leading edge by liquid crystal thermography.

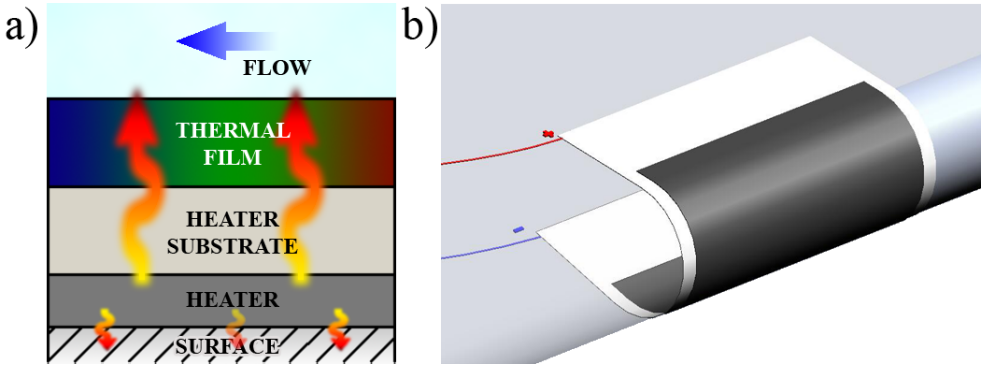

Figure 4: Schematic layout of temperature-sensitive coating (a), and its position at the leading edge of the oblique wing (b)

Ohmic heater power is governed by dimmer to place the film temperature in the operating range. In [17] was found that the overheating of the surface on a methodical 10-15°C did not affect on the cross-scale structures. There is a good agreement of the liquid crystal thermography and thermoanemometry results. The scales of the structures are coincided. Areas with high average speed (heatsink) correspond to the region of low surface temperature, and vice versa. Nevertheless, it is desirable to minimize overheating of the surface by selecting appropriate start working temperature range of the film.
Since the specific heat capacity is constant, the increase in heat transfer leads to decrease of the liquid crystal film temperature, and conversely. The resulting color rendering (heat signature of near-wall flow structure) is recorded with a digital camera to computer, and then the temperature field can be restored.
The camera position was chosen to minimize the angular dependence of the color liquid-crystal film, and maximize visualization area, and not to affect on the studied flow.
It is necessary to highlight some features of liquid crystal thermography:
- informative rapid diagnosis and reusable;
- high spatial resolution and temperature sensitivity;
- a model should made of a heat insulator or there should be thermal isolation on the model of metal to avoid the spreading of heat;
- in a subsonic flow with small temperature changes it needs quality ohmic heater with a uniform distribution of heat power. Nonuniformity of heat flux can be controlled by the LC coating color in experiments without flow;
- the need for a quality digital camera for accurate film color calibration in the experimental conditions to obtain quantitative data on the temperature;
- inertia reach a steady wing structure temperature is about 20-30 minutes;
- the cholesteric liquid crystals response time on the step heat exposure is from 30 to 200 ms depending on the composition of [18];
- a graphic visualization of the stationary disturbances
Despite the limitations, the technique of liquid crystal thermography is a very convenient tool for the qualitative analysis of stationary structure of the near-wall flow.
Processing pictures of visualization, which will be further referred to as the method of subtraction, consisted of four stages. First, trim unwanted information (areas that lie outside the field of measurement). To highlight the disturbance the difference between perturbed and unperturbed flow pattern was calculated. The picture was processed a median filter with a window 3x3 pixels to remove high frequency noise. The final stage is carrying out normalization of brightness.

3. Vortex structures appearance and first stages of developing

3.1. Conditions of disturbance appearance and development

Blowing through a hole on the leading edge of the wing forms a stationary longitudinal vortex disturbance. The airjet in such conditions works as an obstacle for the flow, so it is a certain analogy with the roughness. Depending on the relative position of the hole for blowing and attachment line, disturbance is propagated on one or other surface of the wing. Adjust the speed of injection can change the amplitude and behavior of the longitudinal disturbance, in particular the propagation path. It is because of highly three-dimensional structure near the attachment line, so depending on the strength of blowing the airjet reaches the different height from the surface, where the different direction of the velocity vector, thus the disturbances propagates in different directions, at least in the initial stage of development. Change of created velocity defect value by blowing, influence on the vorticity intensity. It has been considered two modes of injection: u/U_0 = 5%

(small amplitude) and u/U_0 = 8% (large amplitude) (**Fig.11**), Despite a slight difference between the amplitudes of the perturbations, they are qualitatively different. The relative position between the point injection and attachment line was adjusted to stay disturbance on the leading edge as much as possible and propagate on defined side of the wing.

To define the flow conditions hot-wire measurements were carried out on the oblique wing leading edge boundary layer on the attachment line (**Fig.5**). Received velocity profiles analysis showed the constant boundary layer thickness on the attachment line and equals δ = 0.9 mm and the speed in out of boundary layer was U_0 = 3.5 m/s. Reynolds number, calculated using displacement boundary layer thickness, equals in these conditions Re = 58.6.

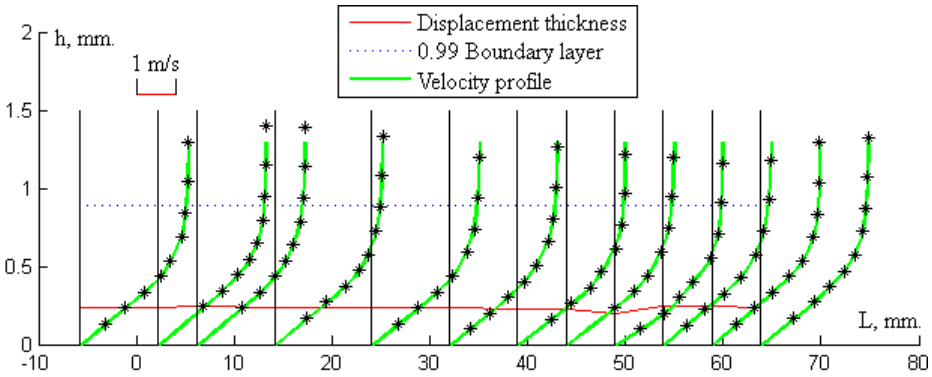

Figure 5: Velocity profiles, displacement thickness and 0.99 boundary layer thickness on the attachment line of an oblique wing.

3.2. Small amplitude regime

The next step was pneumoroute adjusting in small amplitude regime to highlight artificial velocity disturbances on the background noise and minimize them simultaneously. Velocity defect on the 5 mm distance from the source was 5% of velocity component, tangent to attachment line, of upper layers of boundary layer. Then, high frequency disturbances of different frequencies were introduced jointly with stationary disturbance, and investigated the frequency response of the compressor-pneumoroute system, (**Fig.6**).

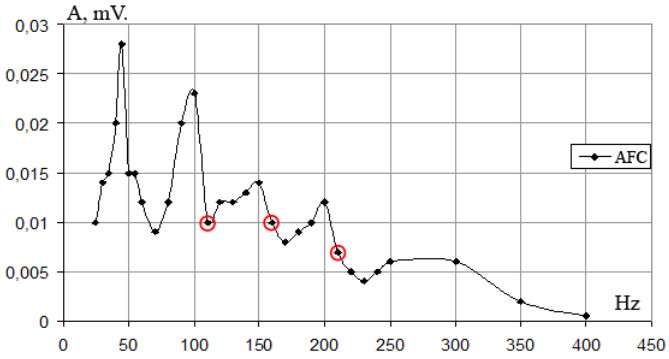

Figure 6: Frequency response of the compressor-pneumoroute system on 5 mm distance from the source of disturbances.

The frequencies that are multiples of 50 Hz was allowed maximum, but in terms of noise, these frequencies are unfavorable, because all devices are powered by a 50 Hz and including a compressor used. For further measurements were selected frequencies separated from the resonance: 110 Hz, 160 Hz and 210 Hz.

Velocity disturbance distributions by Z in regimes with and without superposition of high-frequency disturbances near and far from the blowing source are the same, thus the injected high-frequency perturbations does not affect the mean flow, which speaks about linearity of them.

For a more detailed analysis of the quasi-stationary and high frequency disturbances disturbances behavior hot-wire measurements were carried out on a flat grid parallel to the Z axis and the leading edge of a swept wing, with and without superposition of high-frequency disturbances. After the data processing have been received the stationary velocity disturbance distribution (**Fig.8**), the amplitude of the high frequency disturbance (**Fig.9**), the standard deviation of the natural (**Fig.14**) and artificial high-frequency disturbances.

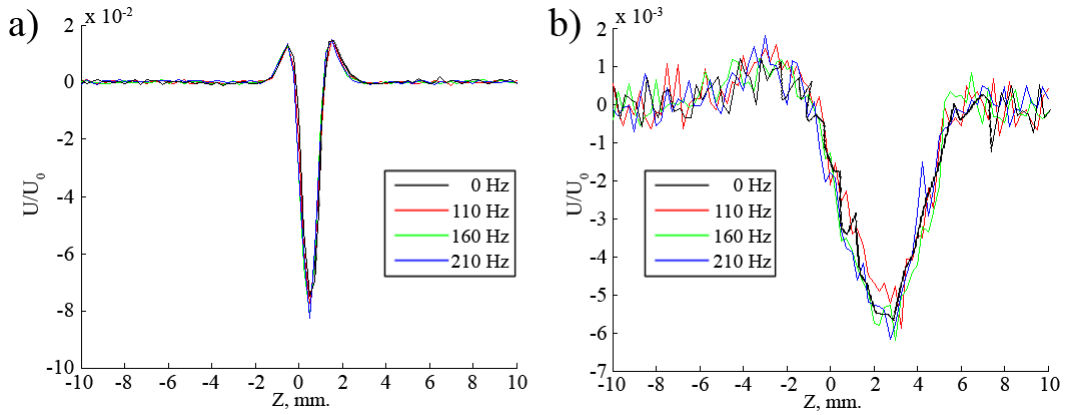

Figure 7: Velocity disturbance distribution for several frequency of injected perturbations on 5 mm distance from the blowing source (a) and 25 mm (b)

From the analysis of the stationary velocity disturbance has been shown that in experiment stationary vortices propagate on both sides from the attachment line (**Fig.8**) This is a redistribution of power between the two vortices in accordance with the relative positions of disturbance source and attachment line. In the measurement area stationary disturbances don't grow along the propagation.

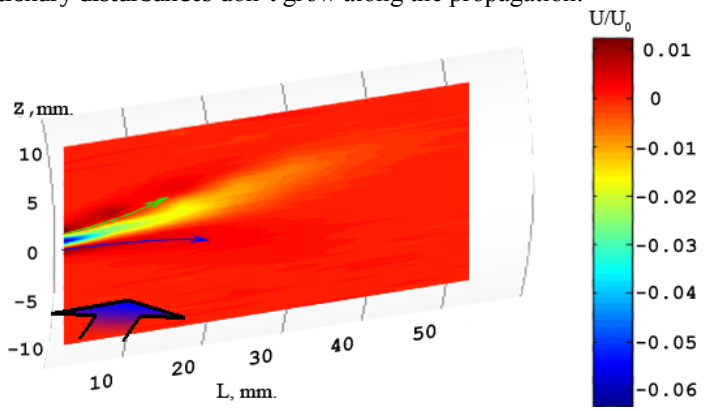

Figure 8: Velocity disturbance distribution on the flat along the leading edge in small amplitude regime.

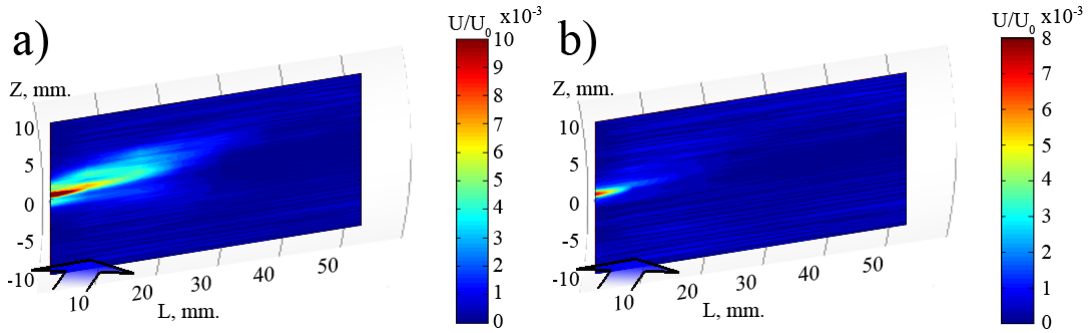

Figure 9: High-frequency disturbance amplitude distribution on the flat along the leading edge in superposition with stationary mode (a) and without stationary mode (b).

Introduced high frequency disturbances decay rapidly. It was found that decrement in the disturbed area is less (**Fig.9.a**, **Fig.10.a**) than in the undisturbed (**Fig.9.b**, **Fig.10.b**), so the high frequency disturbances are distributed together with the stationary (**Fig.9.a**). Comparative analysis of the decay rate revealed that with increase frequency decay rate increases (**Fig.17**).

Character of natural pulsations distribution at small amplitude stationary disturbance (**Fig.14.a**) did not reveal the special role of stationary disturbances in their growing and the formation of secondary instability, there is no growth of the natural fluctuations.

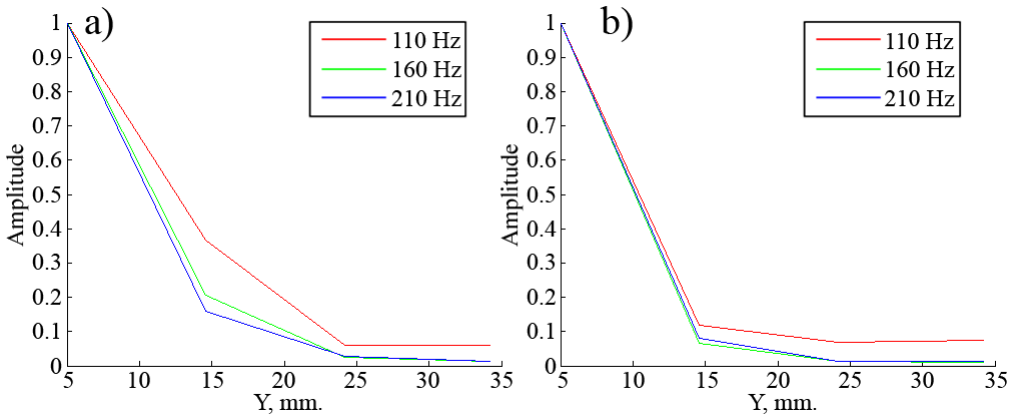

Figure 10: High-frequency disturbance decaying along the oblique wing leading edge superposed with stationary mode (a) and without stationary mode (b).

3.3. High amplitude regime

The next step was adjusting pneumoroute to the large amplitude regime. Velocity defect at a distance of 5 mm. from the source of disturbance was 8% (**Fig.11**) of the along the leading edge velocity component. The transverse size of the vortex disturbance is three times the size of the small amplitude vortex. Hot-wire measurements were carried out on a flat grid (**Fig.2.b**) parallel to the axis Z and the oblique wing leading edge and in volume (**Fig.2.a**) formed of seven planes that are parallel to the leading edge and orthogonal to the cylinder surface. After processing the data were constructed velocity disturbance distribution (**Fig.12**), velocity pulsations in the plane and in the volume (**Fig.13**).

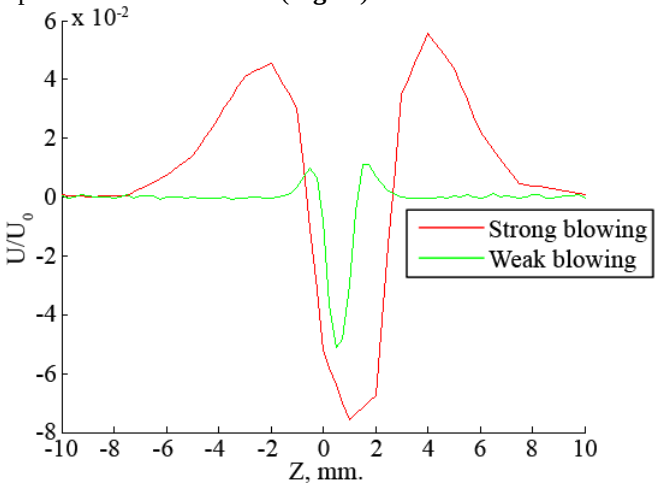

Figure 11: Velocity disturbance distribution on 5 mm distance from the source for small (green) and high (red) amplitude regimes.

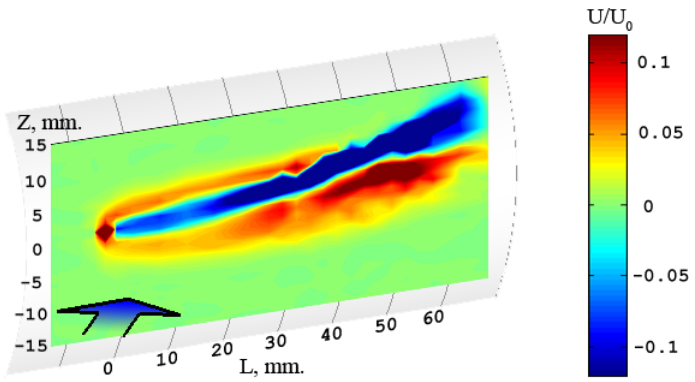

Figure 12: Velocity disturbance distribution on the flat along the leading edge in high amplitude regime.

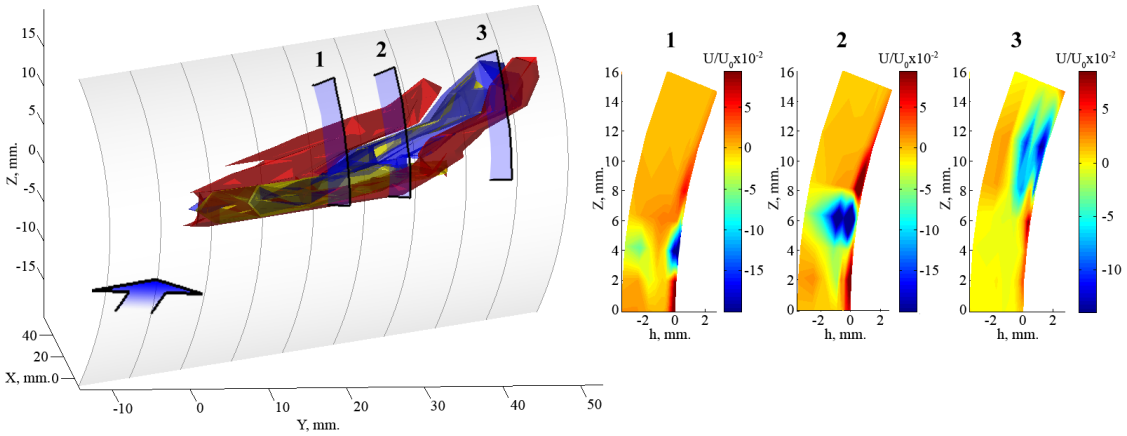

Figure 13: Isosurfaces of exceeding $6.3*10^{-3}U_0$ (red), defect $3.5*10^{-2}U_0$ (blue), standard deviation of velocity $7.9*10^{-3}U_0$ (yellow) and velocity disturbance distribution in three sections.

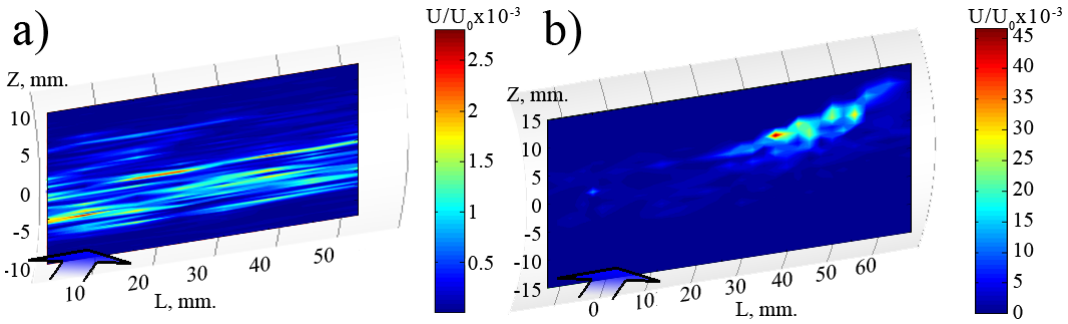

Figure 14: Pulsations distribution on the flat along the oblique wing leading edge in small (a) and high (b) amplitude regimes of excited stationary disturbance.

Analysis of the defect and exceeding velocity distribution showed that the steady velocity perturbation propagates in the same side of the attachment line and increases along the downstream (**Fig.12**). The velocity disturbance distribution pattern indicates the presence of two counter-rotating longitudinal vortices, one of which begins to dominate downstream (**Fig.13**).

The velocity pulsation distribution character (**Fig.14.b**) shows a presence of favorable conditions for natural disturbance development and appearance of secondary instability in disturbed zone, in defect of velocity area mostly.

3.4. Liquid crystal thermography visualization pictures

Changing the point of disturbance injection relative to the attachment line leads to a change in the trajectory of stationary disturbance (**Fig.15**). The increase angle between disturbance source and attachment line leads to increase angle between the initial trajectory of the disturbance and attachment line and make lower transverse dimension of stationary vortices. The first is because excited disturbances are longitudinal and propagate along the streamlines.

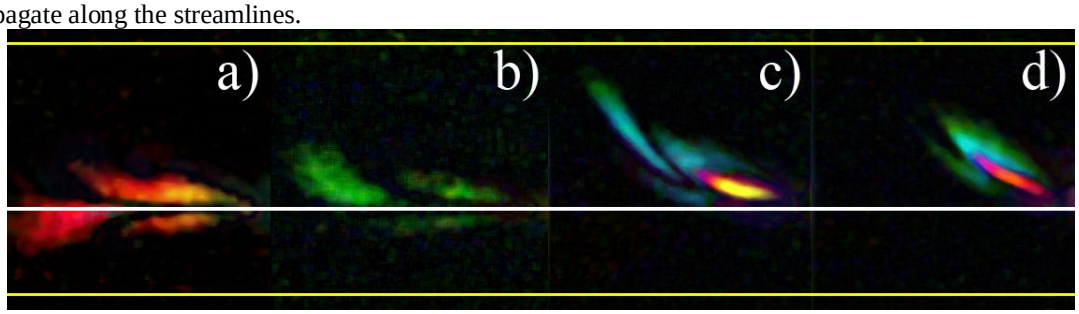

Figure 15: Visualization pictures of stationary disturbance by subtraction method for different blowing source location relative to the attachment line (white line): α = -0.16°, d = -0.1 mm (a), 0.16°= 0.1 mm (b), 1.13° = 0.8 mm (c), 2.59° = 1.8 mm (d). The freestream velocity is 3.4 m/s. Yellow lines are visible boundaries of cylinder which defines the leading edge.

In the case where disturbance exciting point is close to the attachment line, there is a chaotic vortex stall in one direction of it (**Fig.15.a**), or the other (**Fig.16.b**, **Fig.16.c**). Probably, in this case, the disturbance trajectory becomes sensitive to blowing.

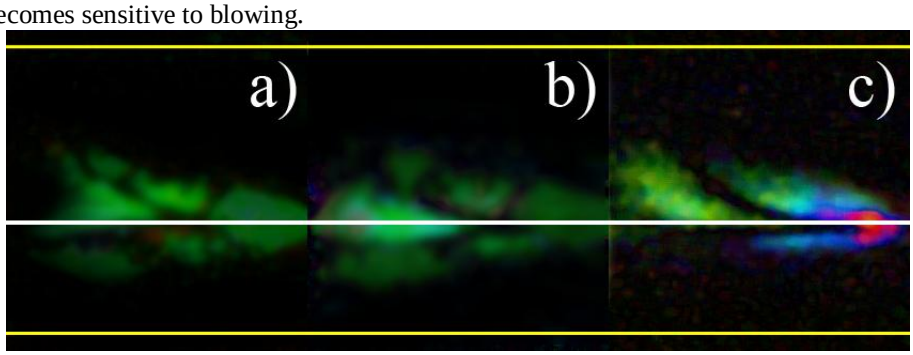

Figure 16: Visualization pictures of stationary disturbance by subtraction method for blowing source location near to the attachment line (white line). The freestream velocity is 3.4 m/s. Yellow lines are visible boundaries of cylinder which defines the leading edge.

The next step was to study the influence of the blowing velocity on the stationary mode behavior. Not to change the disturbance trajectory, the blowing point was offset from the attachment line.
Increasing the blowing speed (**Fig.17**) increases the amplitude of the stationary disturbances, its transverse dimension and a small change in the propagation path – the angle between disturbance trajectory and attachment line become smaller, which can caused by interaction between stationary vortices and surface.

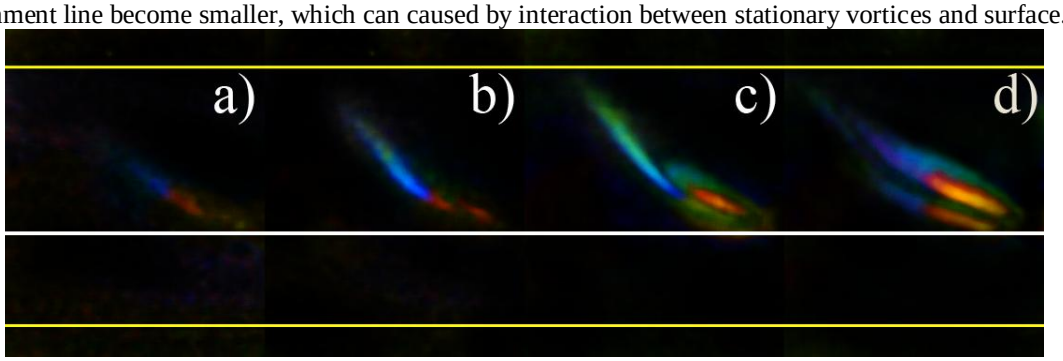

Figure 17: Visualization pictures of stationary disturbance by subtraction method for blowing source located on 1.24 mm from the attachment line (white line). Blowing velocity is: 0.8 m/s (a), 1.1 m/s (b), 2.5 m/s (c), 13.8 m/s (d). The freestream velocity is 3.4 m/s. Yellow lines are visible boundaries of cylinder which defines the leading edge.

In one blowing regime multiplication was observed (**Fig.18**), instead of two counter-rotating vortices, there was born four. There could be two explanations. The first is that airjet from the hole interacts with the oncoming flow in the boundary layer in complex way and excites four vortices instead of two. This situation isn't typical for the flow after roughness element. The second explanation is that the trajectory of the pair of stationary disturbances is very sensitive to the blowing velocity pulsations in the compressor, creating the illusion of four vortices on the visualization picture.

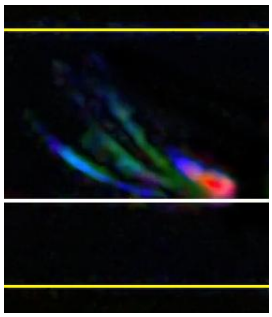

Figure 18: Visualization pictures of stationary disturbance by subtraction method for blowing source located on 1.24 mm from the attachment line (white line). Blowing velocity is 11.6 m/s. The freestream velocity is 9.4 m/s. Yellow lines are visible boundaries of cylinder which defines the leading edge.

We should highlight the strong blowing regime (**Fig.19**) in which the compressor was running at full power, but the jet velocity through the hole is unknown because the flowmeter was not designed for such flow rate (V_{jet} >> 16 m/s). On visualization there is a wide disturbance tail caused by non-linear processes in the modified flow.

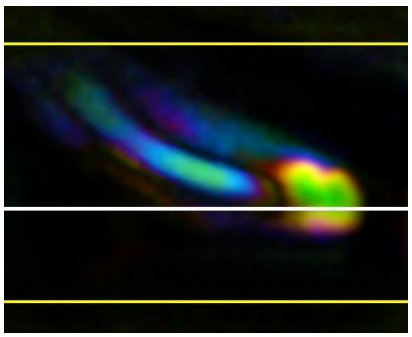

Figure 18: Visualization pictures of stationary disturbance by subtraction method for blowing source located on 1.24 mm from the attachment line (white line). Blowing velocity is bigger than 16 m/s. The freestream velocity is 3.4 m/s. Yellow lines are visible boundaries of cylinder which defines the leading edge.

4. Conclusions

4.1. Thermoanemometry

Investigations on the oblique wing leading edge carried out in two blowing regimes and different measurement grids with a help of controlled disturbance technique. Hot-wire measurements showed constant boundary layer thickness on the attachment line, which allows not taking into account boundary effects in measurement area because of the limit wingspan. Spatial stationary disturbance distribution shows the existence of two counter rotating longitudinal vortices. The zero mode behavior depends on the velocity defect, created by blowing through the small hole. In small velocity blowing regime there is no stationary disturbance growing. Investigations of linear high-frequency disturbances and their interaction with stationary mode showed decrease of their amplitude along the stream and lower decay rate in superposition with stationary mode regime. The increase of frequency leads to the growing decay rate. In high velocity blowing regime there was growing along the stream of stationary disturbance, secondary disturbances and natural pulsations.

4.2. Liquid crystal thermography technique

Results of liquid crystal thermography visualization are in a good agreement with the hot-wire measurements. The stationary point blowing in the boundary layer generates a pair of counter-rotating vortices, and the amplitude of the transverse size of which depend on the blowing strength.
Availability of receiving visualization pictures in a wide range of adjustable parameters allowed to define the influence of the injection velocity on the stationary disturbance trajectory - with increasing injection velocity decreases the angle between the path and the attachment line, which may be due to the interaction of the stationary vortex with the wall. There is observed the instability of stationary disturbance trajectory when the source of the disturbance is located close to the attachment line - one of the vortices is travelled from one side from the attachment line to another. In one regime of blowing on the visualization picture was found four tracks from stationary disturbances, which could say about complex interaction of the airjet with the

incoming flow in boundary layer conditions. Very strong blowing led to the formation of a wide disturbance, size of which is virtually unchanged, indicating the highly non-linear character.
Common result of the work is that weak blowing can be used as the instrument for the boundary layer investigation on the leading edge of the oblique wing. Strong blowing leads to complicate character of the flow and appearance of strong nonlinear effects and could be investigated independently, results of which could be used for the flow control and solving ice formation problems.

5. Acknowledgements

This work was supported by the Russian Foundation for Basic Research, grant №12-01-31347.

6. References

[1] *Blackwelder R. F.* Analogies between transitional and turbulent boundary layers. // Phys. Fluids. – 1983. – Vol. 27(6). – P. 1345 – 1347.
[2] *Reed H. L., Saric W. S.* Stability of three-dimensional boundary layers. // Ann. Rev. Fluid Mech. – 1989. – Vol. 21. – P. 235 – 284.
[3] *Orszag S. A., Patera A. T.* Secondary instability of wall-bounded shear flows. // J. Fluid Mech. – 1983. – Vol. 128. – P. 347 – 385.
[4] *Zhigulyev V. N., Tumin A. M.* Возникновение турбулентности. // Динамическая теория теория возбуждения и развития неустойчивости в пограничных слоях. – Новосибирск: Наука, 1987.
[5] *Kohama Y.* Some expectation on the mechanism of cross-flow instability in a swept-wing flow. // Acta Mech. – 1987. – Vol. 66. – P. 21 – 38
[6] *Poll D.I.A.* Some observations on the transition process on the windward face of a long yawed cylinder // J. Fluid Mech. – 1985. – Vol. 30. - P. 329 – 356.
[7] *Nishizawa A., Tokugawa N., Takagi S.* Experimental investigation of the flow instability near the attachment-line boundary layer on a yawed cylinder //Fluid Dyn. Res 41 (2009) 035513
[8] *Zharkova G.M., Sonin A.S.* Жидкокристаллические композиты. // Новосибирск: Наука Сиб.отд-ние, 1994., 214 с.
[9] *Zharkova G.M., Kovrizhina V.N., Hachaturyan V.M.* Экспериментальное исследование дозвуковых течений методом жидкокристаллической термографии. // ПМТФ, т.43, №2. 2002. с.122-128
[10] *Kozlov V.V., Grek G.R., Litvivnenko M.V., Litvinenko Yu.A., Kozlov G.V.* Круглая струя в поперечном сдвиговом потоке (обзор). // Вестник НГУ. Серия: Физика. 2010. Том 5, выпуск 1., стр. 9.
[11] *Bagheri S., Schlatter Ph., Schmid P. J., Henningson D. S.* Global Stability of Jet in Cross-Flow // J. Fluid Mech. 2009. Vol. 624. P. 33–44.
[12] *New T. H., Lim T. T., Luo S. C.* Effects of Jet Velocity Profiles on a Round Jet in Cross-Flow // Experiments of Fluids. 2006. Vol. 40. No. 3. P. 859–875.
[13] *Bakchinov, A.A., Westin, K.J.A., Kozlov V.V., & Alfredsson, P.H.* Experiments on localized disturbances in a flat plate boundary layer. Part 2 Interaction between localiozed disturbances and TS-waves // Eur. J. Mech./Fluids 17, pp. 847-873. 1998
[14] *Bakchinov A.A., Grek G.R., Katasonov M.M., and Kozlov V.V.* Experimental investigation of the interaction of longitudinal streaky structures with a high-frequency disturbance// Fluid Dynamics, Vol. 33, No. 5, 1998, pp. 667-675.
[15] *Grek G.R., Katasonov M.M., Kozlov V.V., Chernoray V.G.* Моделирование “пафф”- структур в двух- и трехмерных пограничных слоях // Новосибирск, 1999. – (Препр. / РАН. Сиб. отд-ние. Ин-т теор. и прикл. механики; № 2-99).
[16] *Zharkova G.M., Kovrizhina V.N., A.P. Petrov A.P., Shapoval, E.S., Mosharov V.E. and Radchenko V.N.* Visualization of boundary layer transition by shear sensitive liquid crystals.// Proc. PSFVIP-8: The 8th Pacific Symposium on Flow Visualization and Image Processing,- August 21st-25th, 2011 Moscow, Russia. No. 113. - P. 1-5. ISBN 978-5-8279-0093-1
[17] *Brylyakov A.P., Zharkova G.M., Zanin B. Yu., Kovrizhina V.N., Sboyev D.S.* Влияние турбулентности набегающего потока на структуру течения на клине и наветренной стороне профиля. // ПМТФ. – 2004. – т.45, №4. - с.64 -71.
[18] *P T Ireland and T V Jones* The response time of a surface thermometer employing encapsulated thermochromic liquid crystals. // 1987 *J. Phys. E: Sci. Instrum.* 20, 1195